Investigation of enhanced gas absorption by adsorptive bucky balls in a multiphase slurry reactor in the presence and absence of ultrasound

Dagaonkar, M.V.; Heeres, Hero; Beenackers, A.A C M; Pangarkar, V.G.

Published in:
Industrial & Engineering Chemistry Research

DOI:
10.1021/ie010628y

Publication date:
2002

Investigation of Enhanced Gas Absorption by Adsorptive Bucky Balls in a Multiphase Slurry Reactor in the Presence and Absence of Ultrasound

M. V. Dagaonkar,[†] H. J. Heeres,*[,†] A. A. C. M. Beenackers,[†,‡] and V. G. Pangarkar[§]

Department of Chemical Engineering, University of Groningen, Nijenborgh 4, 9747 AG Groningen, The Netherlands, and Department of Chemical Engineering, University of Mumbai, N. M. Parekh Marg, Matunga, Mumbai 400019, India

Fullerenes (e.g., bucky balls) constitute a fascinating class of novel materials, which have shown very high adsorption capacities for hydrogen (5−10 wt % at pressures of less than 1 bar near room temperature by the single-wall nanotubes) under gas−solid conditions. In this work, hydrogen absorption in aqueous slurries of bucky balls has been investigated in a flat stirred cell under slurry conditions at different solid loadings in the presence and in the absence of ultrasound. Enhancements in the gas absorption up to 2.4 were observed using suspended bucky balls. Further enhancements could be obtained by application of ultrasound during the experiment or by presonication of the slurry. Gas absorption rates are a strong function of the solid loading and the stirrer speed. The performance of the bucky balls was compared to that of activated carbon. Bucky balls showed a higher adsorption capacity for H_2 than activated carbon. The increase in the gas absorption in the presence and in the absence of ultrasound was theoretically analyzed using the enhanced gas absorption model. Good agreement between observed and theoretical enhancement factors was obtained.

1. Introduction

Gas-to-liquid mass-transfer rates in three-phase gas−liquid−solid (G−L−S) systems may be enhanced dramatically when the solid phase consists of small particles. This effect may be due to adsorption of the component to the particles or catalysis by the particles or by chemical reactions involving the particles. Several reviews have appeared in the literature which have summarized the results of various experimental and theoretical studies.[1−13] A significant number of studies are concerned with the physical absorption of gaseous reactants in aqueous slurries of carbon-based materials such as activated carbon and noble metal catalysts on a carbon carrier. Enhancement factors in the range of 2−3 were observed for small particles with a high affinity for the substrate to be transferred.[14] In all cases, enhancement levels are a function of the particle loading. After a minimum loading, the enhancement levels off and reaches a constant maximum level. A number of theories have been developed to explain the experimental observations.

Recently, the storage of hydrogen in carbon materials has attracted renewed attention because of the availability of novel carbon nanomaterials, i.e., fullerenes (e.g., bucky balls), nanotubes, and nanofibers.[15−22] These authors have investigated the storage capacity of these new carbon-based materials for gaseous hydrogen, both theoretically and experimentally in the absence of liquid media. Very high adsorption capacities for hydrogen (5−10 wt % at pressures of less than 1 bar near room temperature by the single-wall nanotubes) under G−S conditions have been observed.

However, data on the adsorption of H_2 by the bucky balls have been very much restricted to the G−S systems, and gas absorption under slurry conditions has not been reported so far. Being micron or even smaller sized and having a high affinity for hydrogen in dry conditions, a high partition coefficient and thus higher enhancements might also be expected under slurry conditions. Hence, the objective of the present work is to investigate the effect of a typical fullerene (bucky balls, C60) on mass transfer of hydrogen in aqueous slurries and to compare its performance with that of activated carbon.

2. Experimental Section

The experiments were carried out in a thermostated reactor of glass and stainless steel as shown in Figure 1. A six-bladed turbine stirrer was located centrally in the liquid at a height above the reactor bottom equal to half of the reactor diameter. Four symmetrically mounted glass baffles increased the effectiveness of stirring and prevented the formation of a vortex. The pressure and temperature transducers together with valves 1 and 2 were connected to an Olivetti M240 computer, thus enabling automatic data collection and programmed reactor operation. The dimensions of the reactor and ultrasound horn are given in Table 1. A Branson Ultrasonic disruptor sonifier W-450 with a frequency of 20 kHz and a maximum power output of 400 W was used for carrying out the experiments under ultrasound. The entire assembly of the sonifier was fixed into the stainless steel lid of the reactor, as shown in Figure 1. The horn made of titanium (tip diameter of 0.013 m; surface area of the tip = 1.13×10^{-4} m^2) was dipped approximately 0.035 m into the suspension of bucky

* Corresponding author. Tel: (+)31-50-3634174. Fax: (+)31-50-3634479. E-mail: H.J.Heeres@chem.rug.nl.
[†] University of Groningen.
[‡] Deceased on April 19, 2001.
[§] University of Mumbai.

10.1021/ie010628y CCC: $22.00
Published on Web 02/26/2002

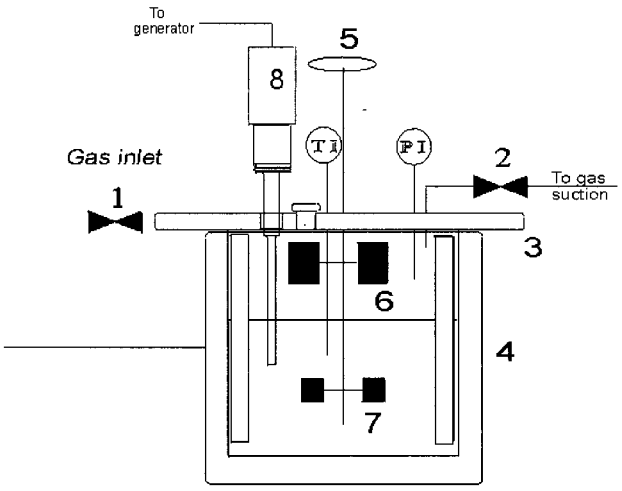

Figure 1. Experimental stirred cell with sonifier (1, gas inlet valve; 2, gas outlet valve; 3, stainless steel reactor lid; 4, glass reactor; 5, stirrer motor; 6, stirrer for the gas phase; 7, stirrer for the liquid phase; 8, sonifier).

Table 1. Reactor and the Ultrasound Horn Dimensions:

Reactor	
diameter	0.105 m
volume	1.777×10^{-3} m^3
G−L contact area	8.37×10^{-3} m^2
liquid impeller type	six-bladed turbine, 0.04 m diameter
gas impeller type	six-bladed turbine, 0.06 m diameter with enlarged six blades
Ultrasound Horn	
tip diameter	0.013 m
surface area	1.13×10^{-4} m^2
frequency	20 kHz
maximum output	400 W

Table 2. Properties of Bucky Balls (As Supplied by Bucky USA)

mean size	7.5×10^{-6} m (in an aqueous suspension, as measured by a Coulter Counter)
specific gravity	1.5−1.7
solubility in water	insoluble
appearance	dark granular solid

balls in the glass reactor and was at a fixed distance of about 0.005 m away from the reactor wall. The particle sizes of the adsorptive particles were measured by a Coulter Counter Multisizer II.

The bucky balls used in the study were as supplied from Bucky USA. The physical properties of the bucky balls are listed in Table 2. The activated carbon was supplied by Norit BV, Amersfoort, The Netherlands. The mean particle size in the slurry conditions as measured by the Coulter Counter were 7.5 μm for the bucky balls and 3.5 μm for the activated carbon particles at a solid loading of 4 kg/m^3.

All of the experiments were carried out batchwise, with respect to both the gas phase and the slurry solution, and new particles were used in each experiment. The volume of the slurry loaded in the reactor was always kept at 1×10^{-3} m^3, and the slurry concentration was varied from 0 to 5 kg/m^3. In a typical experiment without ultrasound, the reactor was filled with the desired slurry (activated carbon/bucky balls dissolved in distilled water) and degassed by opening valve 2 and closing valve 1. Once the slurry was equilibrated under the vapor pressure of water, valve 2 was shut and H_2 was fed to the reactor up to a fixed pressure (0.09 MPa) by opening valve 1. When the pressure reached 0.09 MPa, valve 1 was shut, the stirrer was started, and the decrease of pressure due to the physical absorption of H_2 was recorded over time. The operating conditions of the reactor are listed in Table 3.

Table 3. Experimental Conditions and Physical Data:

temperature	25 °C
initial pressure	0.09 MPa
liquid volume	1×10^{-3} m^3
gas	H_2 purity > 99.5%
stirrer speed	3−12 s^{-1}
D_{AB}	3.6×10^{-9} m^2/s [13]
ρ_{PG} (bucky balls)	1500 kg/m^3 (as supplied by Bucky USA)
ρ_{PG} (activated carbon)	956 kg/m^3 (as supplied by Norit)
He	0.019 [13]

Absorption of hydrogen in the presence of ultrasound was carried out in two ways.

(a) In the first type of experiments, the slurry of known solid loading was put in the stirred cell and irradiated for about 20 min during the degassing procedure and the sonication was also continued during the gas absorption experiments. In the case of high-intensity ultrasound horns, there is a possibility of overheating of the tip. Therefore, the sonication was programmed so that, in a given cycle of sonication, ultrasound irradiation was done for 90% of the cycle. The resulting 10% cycle time was used for cooling of the horn. The power input was adjusted to 20 W. Cold water was circulated through the reactor jacket to maintain a constant temperature of the reactor contents.

(b) In the second type of experiments, instead of sonifying the whole slurry during gas absorption, a presonication procedure was applied. Small volumes of slurries (5×10^{-5} m^3 water with a similar solid loading range of 0−5 kg/m^3) were presonicated in a test tube for 1 h in the absence of hydrogen. The sonication was in a continuous mode, and the duty cycle was 40% (as described above). The objective behind presonication was to segregate the particles. After sonication, the suspension was transferred to the stirred cell setup and mixed with water (to make the total reaction volume of 1×10^{-3} m^3) and then was used for gas absorption experiments. There was no sonication during the experiment.

The particle diameter was determined at the beginning and at the end of each experiment.

3. Gas Solubility and Mass-Transfer Coefficients

The solubility of a gas A in a liquid, defined as the Henry coefficient, is expressed by

$$H = (p_A / C_A^{\,i})_{\text{at equilibrium}} \tag{1}$$

In the absence of a chemical reaction, Henry's constant may be calculated from the experimental data using the following equation:

$$H = \frac{p^\infty - p^{H_2O}}{p^0 - p^\infty} \frac{RTV_L}{V_G} \tag{2}$$

Volumetric mass-transfer coefficients were obtained from the physical absorption rate with time. The value of k_La follows from

$$\frac{Q}{Q+1} \ln\left(\frac{p_A^{\,0}}{(Q+1)p_A - kp_A^{\,0}}\right) = k_L a t \tag{3}$$

where

$$Q = \frac{V_G H}{V_L R T} \tag{4}$$

The rate of H_2 absorption in the slurry follows from

$$J_A a = \frac{V_G}{V_L R T}\left(\frac{-\mathrm{d}p_A}{\mathrm{d}t}\right) \tag{5}$$

4. Theory

Gas absorption experiments in slurries containing small hydrophobic particles such as activated carbon and catalysts supported on a carbon carrier (Pd/C and Rh/C) revealed that the enhancement factors depend on the solid concentration at the G−L interface, particle finite adsorption capacity effects, and geometrical factors at the elevated particle concentration close to the interface. Several models have been developed to explain this observed increase in the enhancement for these types of hydrophobic carbon materials. All of them assume a nonuniform distribution of the particles in the liquid phase with a high concentration of the hydrophobic particles at the G−L interface.[7,13,23−28]

Vinke et al.[13] presented an enhanced gas absorption model (EGAM) based on their work on the absorption of H_2 in the aqueous suspensions containing different concentrations of small carbon-supported or alumina-supported catalyst particles. A relation has been presented to calculate the enhancement factor for the initial gas absorption rates from the fraction of the G−L interface covered by the adhering particles and the concentration of the catalyst particles in the slurry.

The EGAM model of Vinke et al.[13] has been used to analyze the present experimental observations because of the close similarities in the liquid media and particle type (both are carbon-based, hydrophobic particles). The theoretical enhancement factor provided by Vinke et al.[13] is given as

$$E = 1 + \zeta\left[\frac{k_{LS}}{k_L}\left(\frac{1 - \exp(-\tau/\tau_0)}{\tau/\tau_0}\right) - 1\right] \tag{6}$$

where

$$k_{LS} = 4D_{AB}/d_p \tag{7}$$

$$\tau = 4D_{AB}/\pi k_L{}^2 \tag{8}$$

and

$$\tau_0 = m d_p{}^2/6\beta D_{AB} \tag{9}$$

ζ is the fraction of the G−L interface covered by the adsorptive particles, k_L is the mass-transfer coefficient of the uncovered part of the G−L interface, and k_{LS} is the mass-transfer coefficient for the covered part of the G−L interface.

The gas adsorption capacity of the particles at the equilibrium is assumed to be governed by the partition coefficient m, which is defined as

$$m = (\text{amount of hydrogen per unit volume of catalyst particles/amount of hydrogen per unit volume of liquid})_{\text{equilibrium}} \tag{10}$$

This may be rewritten as

$$m = \sigma\rho_{PG}/C_G He \tag{11}$$

where σ denotes the quantity of H_2 adsorbed per kilogram of the solids. This property was measured by taking the difference in the quantity adsorbed in the slurry and the quantity adsorbed in the pure solvent devoid of adsorptive particles for the given amount of solid loading under similar hydrodynamic conditions. The values of the physical properties D_{AB}, ρ_{PG}, and He are provided in Table 3. For a spherical particle, β was assumed to approximately equal to $4/\pi$.

The relationship between ζ and the particle concentration C_b in the liquid bulk was derived by proposing a Langmuir-type adhesion isotherm[13]

$$\frac{\zeta}{\zeta_{max}} = \frac{k_a C_b}{1 + k_a C_b} \tag{12}$$

where k_a is the particle-to-bubble adhesion constant, to be found via fitting of the experimental results. The value of C_b was estimated by taking the overall balance of the particles in the reactor assuming that the catalyst particles adhere in a monolayer of thickness d_p to the interface. By this procedure, C_b can be represented by the equation

$$C_b = \frac{C_s - C_{sed} a d_p \zeta}{1 - a d_p \zeta} \tag{13}$$

Substituting the value of C_b in eq 12 results in

$$a d_p(1 + k_a C_{sed})\zeta^2 - (1 + k_a C_s + k_a C_{sed} a d_p \zeta_{max})\zeta + k_a C_s \zeta_{max} = 0 \tag{14}$$

To obtain the values of ζ_{max} and k_a, the experimental enhancement factors were substituted in eq 6 to estimate the values of ζ at different solid loadings. ζ_{max} and k_a were obtained from the estimated ζ values versus the solid loading by curve fitting. The theoretical value of ζ for each solid loading was then estimated using eq 14 by substituting $C_{sed} = 235$ kg/m^3 and the best-fit values of ζ_{max} and k_a.[13]

The experimental enhancement factor was calculated from

$$E = (\text{gas absorption flux in the suspension/gas absorption flux in a particle free liquid})_{\text{similar hydrodynamic conditions}} \tag{15}$$

5. Results and Discussion

5.1. Absorption of H_2 in Aqueous Slurries of Bucky Balls (in the Absence of Ultrasound). Experiments were performed to determine the absorption of H_2 in slurries of bucky balls (average diameter of 7.5 μm) at different solid concentrations (0−4 kg/m^3) and stirring speeds (3.3 and 10.8 s^{-1}). The results are shown in Figure 2. The rate of hydrogen absorption in the presence of bucky balls is significantly higher than that in pure water, and enhancements of up to 2.5 were observed. The enhancements are a function of the bucky ball loading and the speed of agitation.

As is clearly demonstrated in Figure 2, the enhancement increases at higher loading; however, it appears to level off at higher solid loadings. These observations

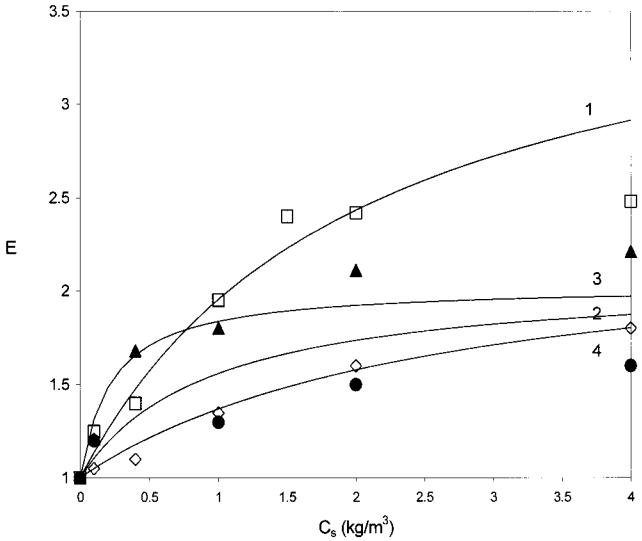

Figure 2. Enhancement factors measured as a function of the particle concentration in the suspension at different stirrer speeds. The solid lines represent theoretical curves for the enhancement factor with best-fit values of k_a and ζ_{max} (H_2−bucky ball slurry: 1, □, 3.3 s^{-1}; 2, ◇, 10.8 s^{-1}; H_2−activated carbon slurry: 3, ▼, 3.3 s^{-1}; 4, ●, 10.8 s^{-1}).

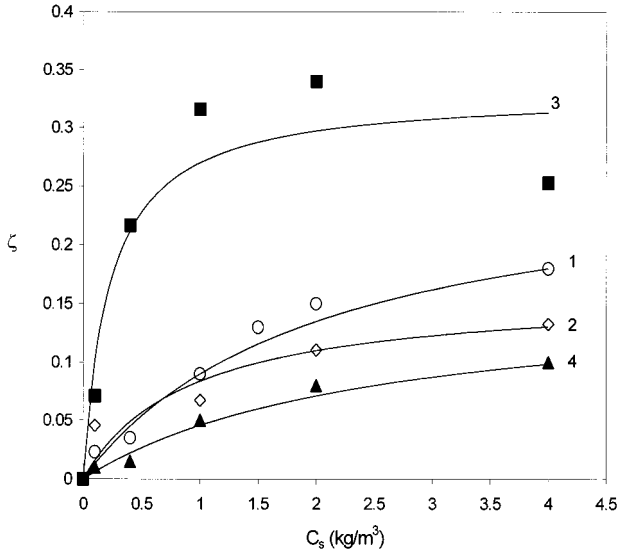

Figure 3. Fraction of bubble-surface coverage ζ plotted as a function of suspension concentration C_s (C_{sed} = 235 kg/m^3)[13] (H_2−bucky ball slurry: 1, ○, 3.3 s^{-1}; 2, ◇, 10.8 s^{-1}; H_2−activated carbon slurry: 3, ■, 3.3 s^{-1}; 4, ▲, 10.8 s^{-1}; solid lines are theoretical predictions).

are in line with experimental observations for other gas-activated carbon slurry systems.[4,6,9] In most cases, the enhancement factor levels off and reaches a constant maximum level, independent of the solid loading. For the bucky-ball experiments, the maximum enhancement levels are outside the experimentally applied range of solid loadings (0−4 kg/m^3).

Vinke et al.[13] have explained the presence of a maximum enhancement factor by assuming a nonuniform distribution of solid particles in the liquid, with a higher solids concentration in the mass-transfer zone than in the bulk liquid. It is assumed that the G−L surface fraction covered by particles may be described by a Langmuir type of adsorption isotherm. Based on this theory, the fraction of the G−L interface covered by the particles will reach a maximum value after a certain minimum solid concentration and, as a consequence, the enhancement factors will attain a maximum value.

The enhancement factors are a function of the stirrer speeds (Figure 2). Enhancement factors are significantly higher at the lower stirrer speed. These effects are related to the differences in the surface fraction covered by particles at various stirrer speeds (refer Figure 3 and Table 4). From Figure 3, it follows that the surface coverage is significantly higher at low stirrer speed. When a Langmuir type of adsorption isotherm is applied for the particles, the value of the surface fraction covered by particles is a function of k_a and ζ_{max}. ζ_{max} is a measure for the surface capacity of the particles, and k_a is a measure for the exchange equilibrium from particles moving to and away from the interface. Both parameters are expected to be affected by the stirrer speed. The value of ζ_{max} decreases at higher stirring intensities, which is in accordance with literature data.

The EGAM model[13] developed for hydrophobic particles was applied to model the experimental data. Theoretical enhancement factors are in reasonable accordance with the experimental data; see Figure 2 for a graphical illustration.

For comparison, similar types of experiments were carried out using active carbon particles. Unfortunately, direct comparison with the bucky balls is not possible because of particle size differences (bucky balls, 7.5 μm; active carbon, 3.5 μm). The results are given in Figure 2. Enhancement factors for the active carbon samples at equal stirrer speeds and solid loadings are on the lower side (more predominantly at higher solid loadings) to those observed for bucky balls.

Table 4. Values of the Adsorption Constant and the Maximum Amount of the Fraction of the G−L Interface Covered by the Adsorptive Particles (ζ_{max})[a]

type of particle	conditions	speed of rotation (s^{-1})	k_a	ζ_{max}
bucky balls	untreated particles	3.3	0.5(0.1)	0.27(0.03)
	untreated particles	10.8	0.4(0.1)	0.16(0.02)
	sonication during experiments	3.3	1.6(0.3)	0.18
	presonicated particles	3.3	37(8)	0.28(0.006)
activated carbon	untreated particles	3.3	4.5(2.5)	0.33(0.04)
	untreated particles	6.7	1.1(0.9)	0.16(0.04)
	sonication during experiments	3.3	1.9(0.4)	0.27(0.02)

[a] Values in parentheses are the standard deviations.

Based on the theoretical model derived by Vinke et al.,[13] a number of parameters may account for these differences between both materials, i.e., the particle surface coverage ζ, the distribution coefficient m, and the particle size diameter. The calculated surface fraction covered by particles as a function of the solid loadings is provided in Figure 3, and the calculated values for ζ_{max} and k_a are given in Table 4. It appears that the values of k_a are slightly higher for activated carbon than for the bucky balls. However, because of the limited amount of data as well as the relatively large errors in the calculated values of ζ_{max} and k_a, it is difficult to draw statistically sound conclusions.

The average particle size diameter of the active carbon samples is lower than those for the bucky balls and, as a consequence, higher enhancement levels are expected for the active carbon samples. In addition, the surface coverage for the active carbon samples, especially at low stirrer speed, is higher than that for the bucky balls, which also would lead to higher enhance-

ment factors. However, this is not the case, and this is mainly because of the differences in the L−S hydrogen partition coefficient, m. The partition coefficient for the H_2−bucky ball slurry system was found to be 225 (±39), and that for the H_2−activated carbon slurry was estimated to be 140 (±14) (average values for six experiments in each case). Hence, bucky balls in aqueous solutions have a higher affinity for hydrogen than active carbon, and this property is the cause of the slightly higher enhancement factors observed for the bucky ball samples (at similar solid loadings).

The modeling studies as well as the experimental data (i.e., the presence of a minimum solids concentration for maximum enhancement) and experimental observations (particle sticking to the G−L interface) suggest that bucky balls are, analogous to active carbon, hydrophobic particles with a high affinity for hydrogen molecules.

5.2. Effect of Ultrasound on the Rate of Gas Absorption. According to the EGAM model, hydrogen enhancement factors are expected to be a strong function of the particle diameter, with smaller particles leading to higher enhancements. It seemed, therefore, worthwhile to reduce the particle size of the bucky ball samples. One of the possible means is the application of ultrasound waves.[29−32] When a S−L interface is subjected to high-intensity ultrasound, acoustic cavitation near the surface induces markedly asymmetric bubble collapse, which generates a high-speed jet of liquid directed at the surface. The impingement of this jet and the related shock waves can create localized erosion of the particle and cause particle fragmentation.

Application of ultrasound during gas absorption might, besides having an effect on the particle sizes, also have an effect on the hydrodynamics near the interface. To study this effect, a number of hydrogen absorption experiments were carried out in the absence of particles. In the absence of particles and at a similar speed of agitation, it turned out that the absorption rate with ultrasound was 2.9 times higher than that in its absence ($J_{H_2,\text{with ultrasound}} = 0.167$ mol/m^2·s, $J_{H_2,\text{without ultrasound}} = 0.07$ mol/m^2·s, as 3.3 s^{-1}). Hence, it appears that the mass-transfer coefficient is positively affected by the presence of ultrasound waves, which is indeed remarkable and is likely due to the creation of additional turbulence near the interface.[29−32] Further experiments beyond the scope of this paper are in progress to address these interesting findings of ultrasound on G−L mass-transfer rates. To compensate for this effect during gas absorption in bucky ball slurries, the enhancement factors for the reactions under ultrasound conditions are defined in the following way:

$$E = (\text{rate of gas absorption in the slurry in the presence of ultrasound/rate of gas absorption in the presence of ultrasound in a particle free liquid})_{\text{similar hydroconditions}} \quad (16)$$

A number of hydrogen absorption experiments in the presence of ultrasound waves were carried out using aqueous slurries of bucky balls and activated carbon. The enhancement factors as a function of the particle loading in the presence of ultrasound are given in Figures 4 (bucky balls) and 5 (active carbon). The enhancement factors at a particular solid loading are only slightly higher than those in the absence of ultrasound. For instance, the enhancement factor for

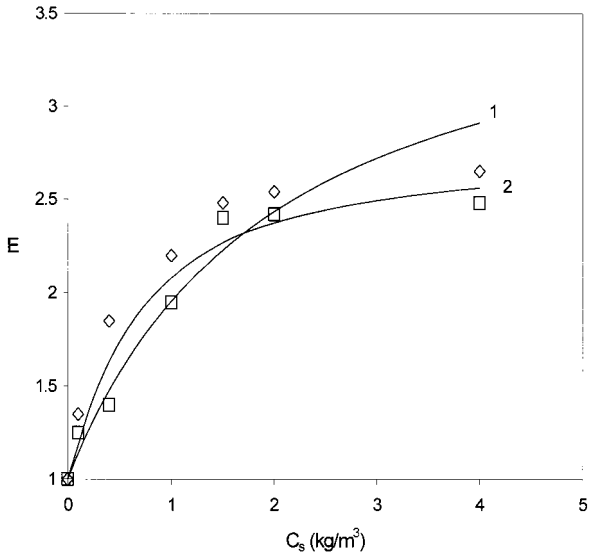

Figure 4. Effect of ultrasound on the enhancement in gas absorption at different solid loadings at 3.3 s^{-1} (H_2−bucky ball slurry: 1, □, no ultrasound; 2, ◇, with ultrasound; solid lines are model curves).

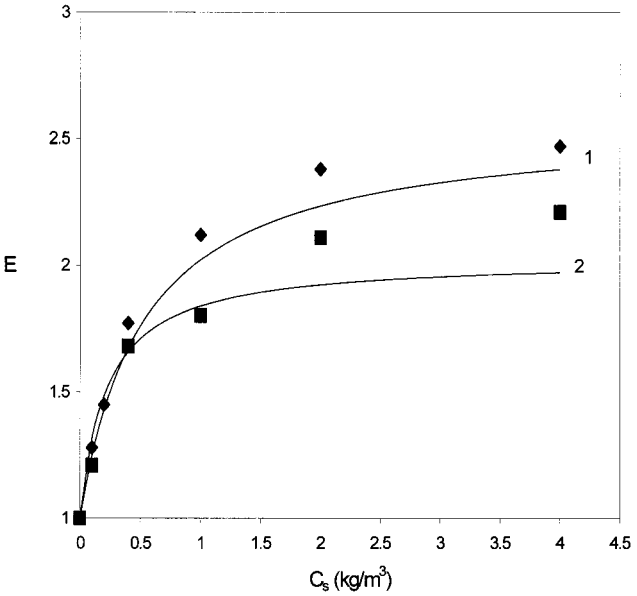

Figure 5. Effect of ultrasound on the enhancement in gas absorption at different solid loadings at 3.3 s^{-1} (H_2−activated carbon slurry: 1, ◆, in the presence of ultrasound; 2, ■, in the absence of ultrasound; solid lines are model curves).

H_2 adsorption by activated carbon was found to be 2.3 and 2.5 in the absence and presence of ultrasound, respectively, as compared to 2.4 and 2.7 for the bucky balls.

The EGAM model predicts that the enhancements are a function of the particle size, the surface coverage ζ, and the partition coefficient m. Data analysis reveals that, as expected, the application of ultrasound does not affect the partition coefficient m. Effects of ultrasound on the particle size distributions were determined by the determination of the particle size distribution before and after an absorption experiment (see Table 5). The particle size of the bucky-ball samples when ultrasound is applied varied between 4.9 and 6.6 μm compared to 7.3 μm for samples in the absence of ultrasound. Hence, ultrasound does affect the particle size distribution in a positive manner (smaller sizes), although the effects

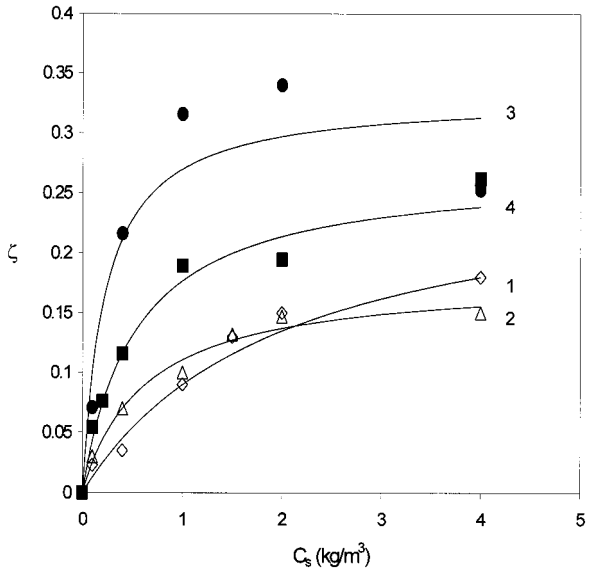

Figure 6. Fraction of bubble-surface coverage ζ plotted as a function of suspension concentration C_s at 3.3 s^{-1} (C_{sed} = 235 kg/m^3)[13] (H_2−bucky ball slurry: 1, △, with ultrasound; 2, ◇, without ultrasound; H_2−activated carbon slurry: 3, ■, with ultrasound; 4, ●, without ultrasound; solid lines are theoretical curves).

Table 5. Average Particle Size of the Bucky Balls

solid loading (kg/m^3)	0.1	0.4	1	1.5	2	4
particle diameters (d_p, μm)						
1. sonication during experiment	4.9	5.8	6.0	6.5	6.5	6.6
2. presonication	3.5	3.8	4.0	4.1	4.1	4.2

are relatively small. As shown in Table 4 and Figure 6, the fraction of the G−L interface covered by the particles is slightly affected when ultrasound is applied during the experiments. However, both of the values of ζ_{max} and k_a at a fixed stirrer speed (Table 4) are statistically similar in the presence and absence of ultrasound. The possible reason for this is that the ultrasonic radiation is directed toward the bottom of the experimental setup. By the time the ultrasound turbulence reaches the G−L interface at the top, it is weakened dramatically and causes only minor disturbances of the G−L−S interface. In conclusion, it appears that the slight increase in gas enhancement when ultrasound is applied is mainly due to a reduction in the average particle size due to the action of ultrasound.

Gas absorption experiments using the presonicated bucky-ball samples resulted in enhancements of up to 3.0, which is significantly higher than those found for the absorption experiments using untreated bucky balls or applying ultrasound during an experiment (Figure 7). Particle size measurements confirm that the presonication procedure is the most efficient way of reducing the average particle size of the bucky-ball samples. The average particle size reduced from 7.5 μm for an untreated sample to 3.5−4.2 μm for presonified samples and 4.2−6.5 μm for samples with sonication applied during the absorption experiments (Table 5). The reduction in particle size is a function of solid loading, with higher loading leading to less size reduction.

The differences in absorption rates due to presonication may, besides particle size effects, also be related to differences in particle surface coverages (Figure 8). The values of k_a and ζ_{max} were determined from the experimental data (Table 4) and found to be significantly different from those obtained in the absence of sonication or using sonication during the experiments. Especially, the value of k_a seems to be significantly higher when using the pretreated samples. Prediction and understanding of the effects of various factors on the surface particle coverage is an area which has not been studied in detail, and literature reports are scarce. Whether the observed differences in surface coverage are particle size related or other particle properties (e.g., the wetting ability) are affected as well is not clear at this stage. The gas absorption experiments using sonication during gas absorption experiments or presonication were modeled using the EGAM theory. Theoretical enhancement factors were calculated using eq 6 and the best-fit values of k_a and ζ_{max}. Agreement between theoretical and observed enhancement factors was reasonably good; see Figures 4, 5, and 7 for details.

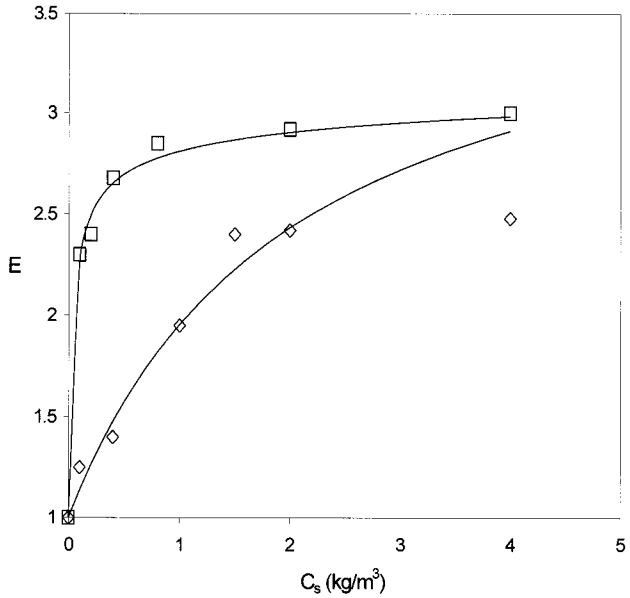

Figure 7. Effect of presonication on the enhancement in gas absorption at different solid loadings at 3.3 s^{-1} (H_2−bucky ball slurry: □, presonicated particles; ◇, nonsonicated particles; solid lines are theoretical curves).

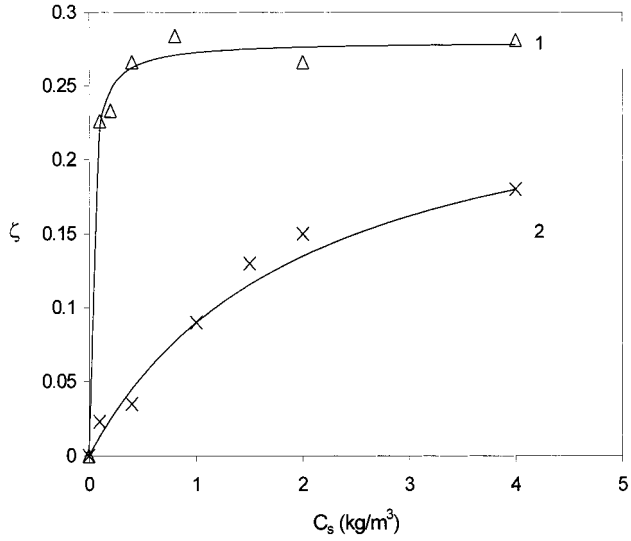

Figure 8. Effect of presonication on the fraction of the G−L interface covered by the adsorptive particles at different solid loadings at 3.3 s^{-1} (H_2−bucky ball slurry: 1, △, presonicated particles; 2, ×, nonsonicated particles; solid lines are theoretical curves).

6. Conclusions

Hydrogen absorption in an aqueous solution may be enhanced by the presence of micron-sized bucky-ball particles. Enhancement factors of up to 2.4 (compared to 2.3 in the presence of activated carbon particles) were observed at room temperature with a solid loading of 4 kg/m^3 at 3.3 s^{-1}. The enhancement is a function of the bucky-ball loading and the speed of agitation. The experimental data and observations as well as the modeling studies suggest that bucky balls are hydrophobic particles with (hydrogen adsorption) properties mimicking activated carbon. Reduction of the average particle size of the bucky balls by a factor of 2 could be achieved by applying ultrasound waves before a gas absorption experiment. This resulted in an increase in the enhancement factor to about 3.0. Besides affecting the particle size dimensions, ultrasound also affects the hydrodynamics in the liquid mass-transfer layer. In the absence of particles, the rate of mass transfer of hydrogen in water was about 3 times higher when ultrasound is applied. Vinke's EGAM model was applied to model the observations. The theoretical enhancement factors are in good agreement with the experimental values.

Acknowledgment

The financial support given by NWO (Netherlands Organization for Scientific Research) is gratefully acknowledged.

Nomenclature

a = G−L interfacial area (m^2/m^3 dispersion)
C_A^i = concentration of A (gas) at the G−L interface (mol/m^3)
C_b = mass of gas-absorbing particles per unit volume of bulk of the suspension (kg/m^3)
C_s = mass of gas-absorbing particles per unit volume of suspension (kg/m^3)
C_{sed} = mass of gas-absorbing particles per unit volume in a sedimented layer (kg/m^3)
C_G = concentration of hydrogen in the gas phase (mol/m^3)
D_{AB} = binary diffusion coefficient of hydrogen in the liquid phase (m^2/s)
d_p = particle diameter (m)
E = enhancement factor
He = Henry number defined as $(C_A^i/C_G)_{equilibrium}$
H = Henry constant (Pa·m^3/mol)
J = rate of gas absorption (mol/m^2·s)
k_a = particle adhesion coefficient (m^3/kg)
k_L = liquid-side mass-transfer coefficient of the uncovered part of the G−L interface (m/s)
k_{LS} = liquid-side mass-transfer coefficient of the covered part of the G−L interface (m/s)
m = partition coefficient as defined in eq 10
p_A = partial pressure of component A in the gas phase (Pa)
Q = constant as defined in eq 4
R = gas constant (J/mol·K)
T = temperature (K)
t = time (s)
V_L = liquid volume (m^3)
V_G = gas volume (m^3)

Superscripts

0 = at time $t = 0$
∞ = at time $t = \infty$

Greek Symbols

ρ_{PG} = density of a solid particle (kg/m^3)
δ_L = stagnant film thickness (m)
σ = amount of hydrogen adsorbed per unit mass of dry catalyst particles (mol/kg)
β = geometrical factor ($=4/\pi$)
ζ = fraction of the G−L interface covered by the adhering solid particles
τ = average residence time of an adhering catalyst particle at the G−L interface (s)

Literature Cited

(1) Lee, Y. Y.; Tsao, G. T. Oxygen absorption into glucose solution. *Chem. Eng. Sci.* **1972**, *27*, 1601.

(2) Chandrasekaran, K.; Sharma, M. M. Absorption of oxygen in aqueous solutions of sodium sulfide in the presence of activated carbon as catalyst. *Chem. Eng. Sci.* **1977**, *32*, 669.

(3) Kars, R. L.; Best, R. J.; Drinkenburg, A. A. H. The sorption of propane in slurries of active carbon in water. *Chem. Eng. J.* **1979**, *17*, 201.

(4) Alper, E.; Wichtendahl, B.; Deckwer, W. D. Gas absorption mechanism in catalytic slurry reactors. *Chem. Eng. Sci.* **1980**, *35*, 217.

(5) Pal, S. K.; Sharma, M. M.; Juvekar, V. A. Fast reactions in slurry reactors: catalyst particle size smaller than film thickness: oxidation of aqueous sodium sulfide solutions with activated carbon particles as catalyst at elevated temperatures. *Chem. Eng. Sci.* **1982**, *37*, 327.

(6) Alper, E.; Deckwer, W. D. *Some aspects of gas absorption mechanism in slurry reactors*; NATO ASI Series E73; Martinus Nijhoff: The Hague, 1983; Vol. 2.

(7) Wimmers, O. J.; Paulussen, R.; Vermeulen, D. P.; Fortuin, J. M. Enhancement of absorption of a gas into a stagnant liquid in which a heterogeneously catalysed chemical reaction occurs. *Chem. Eng. Sci.* **1984**, *39*, 1415.

(8) Alper, E. Kinetics of absorption of oxygen into aqueous solutions of sodium sulfide containing finely powdered activated carbon in a slurry reactor. *Chem. Eng. Commun.* **1985**, *36*, 45.

(9) Alper, E.; Ozturk, S. Effect of fine solid particles on gas−liquid mass transfer rate in a slurry reactor. *Chem. Eng. Commun.* **1986**, *46*, 147.

(10) Wimmers, O. J. The enhancement of gas absorption by a heterogeneously catalysed chemical reaction. Ph.D. Dissertation, University of Amsterdam, Amsterdam, The Netherlands, 1987.

(11) Quicker, G.; Alper, E.; Deckwer, W. D. Gas absorption rates in a stirred cell with plane interface in the presence of fine particles. *Can. J. Chem. Eng.* **1989**, *67*, 32.

(12) Tinge, J. T.; Ende, H. C. O.; Berendsen, H. J. C.; Drienkenburg, A. A. H. The absorption of propane and ethene slurries of activated carbon in water—II. *Chem. Eng. Sci.* **1991**, *46*, 343.

(13) Vinke, H.; Hamersma, P. J.; Fortuin, J. M. H. Enhancement of the gas-absorption rate in agitated slurry reactors by gas-adsorbing particles adhering to gas bubbles. *Chem. Eng. Sci.* **1993**, *48*, 2197.

(14) Beenackers, A. A. C. M.; van Swaaij, W. P. M. Mass transfer in gas−liquid slurry reactors. *Chem. Eng. Sci.* **1993**, *48* (18), 3109.

(15) Dillon, A. C.; Jones, K. M. M.; Bekkedahl, T. A.; Kiang, C. H.; Bethune, D. S.; Heben, M. J. Storage of hydrogen in single-walled carbon nanotubes. *Nature* **1997**, *386*, 377.

(16) Stan, G.; Cole, W. Hydrogen adsorption in nanotubes. *J. Low Temp. Phys.* **1998**, *110*, 539.

(17) Rzepka, M.; Lamp, P.; de la Casa-Lillo, M. A. Physisorption of hydrogen on microporous carbon and carbon nanotubes. *J. Phys. Chem. B* **1998**, *102*, 10894.

(18) Darkrim, F.; Levesque, D. Monte carlo simulations of hydrogen adsorption in single-walled carbon nanotubes. *J. Chem. Phys.* **1998**, *109* (12), 4981.

(19) Chambers, A.; Park, C.; Baker, T. K.; Rodriguez, N. M. Hydrogen storage in graphide nanofibre. *J. Phys. Chem. B* **1998**, *102* (22), 4253.

(20) Chen, P.; Wu, X.; Lin, J.; Tan, K. L. High H_2 uptake by alkali-doped carbon nanotubes under ambient pressure and moderate temperatures. *Science* **1999**, *285*, 91.

(21) Wang, Q.; Johnson, J. K. Molecular simulation of hydrogen adsorption in single-walled carbon nanotubes and idealised carbon slit pores. *J. Chem. Phys.* **1999**, *110* (1), 577.

(22) Ye, Y.; Ahn, C. C.; Withan, C.; Fultz, B.; Liu, J.; Rinzler, A. G.; Colbert, D.; Smith, K. A.; Smalley, R. E. Hydrogen

adsorption and cohesive energy of single-walled carbon nanotubes. *Appl. Phys. Lett.* **1999**, *74* (16), 2307.

(23) Holstvoogd, R. D.; van Swaaij, W. P. M.; van Dierendonck, L. L. The adsorption of gases in aqueous activated carbon slurries enhanced by adsorbing or catalytic particles. *Chem. Eng. Sci.* **1988**, *43*, 2181.

(24) Wimmers, O. J.; Fortuin, J. M. H. The use of adhesion of catalyst particles to gas bubbles to achieve enhancement of gas absorption in slurry reactors- I. Investigation of particle to bubble adhesion using the bubble pick-up method. *Chem. Eng. Sci*. **1988**, *43*, 303.

(25) Wimmers, O. J.; Fortuin, J. M. H. The use of adhesion of catalyst particles to gas bubbles to achieve enhancement of gas absorption in slurry reactors—II: Determination of the enhancement in a bubbles-containing slurry reactor. *Chem. Eng. Sci*. **1988**, *43*, 313.

(26) Karve, S.; Juvekar, V. A. Gas absorption into slurries containing fine catalyst particles. *Chem. Eng. Sci*. **1977**, *45*, 587.

(27) Holstvoogd, R. D.; van Swaaij, W. P. M. The influence of adsorption capacity on enhanced gas absorption in activated carbon slurries. *Chem. Eng. Sci*. **1990**, *45*, 151.

(28) Tinge, J. T.; Drienkenburg, A. A. H. The enhancement of the physical absorption of gases in aqueous activated carbon slurries. *Chem. Eng. Sci*. **1995**, *50*, 937.

(29) Suslick, K. S.; Casadonte, D. J. Heterogeneous sonocatalysis with nickel powder. *J. Am. Chem. Soc*. **1987**, *109*, 3459.

(30) Graff, G. M. Putting chemical reactions on a sound footing. *Chem. Eng*. **1985**, March 18, 22.

(31) Suslick, K. S. Sonochemistry. *Science* **1990**, *247*, 1439.

(32) Thompson, L. H.; Doraiswamy, L. K.; Sonochemistry: Science and engineering. *Ind. Eng. Chem. Res*. **1999**, *38*, 1125.

Received for review July 20, 2001
Revised manuscript received December 19, 2001
Accepted December 23, 2001

IE010628Y